



Capillary penetration mechanism and oil mist concentration of Al₂O₃ nanoparticle fluids in electrostatic minimum quantity lubrication (EMQL) milling

Xuefeng Xu¹ · Tao Lv¹ · Zhiqiang Luan¹ · Yangyang Zhao¹ · Minghuan Wang¹ · Xiaodong Hu¹

Received: 24 November 2018 / Accepted: 17 June 2019 / Published online: 22 June 2019
© Springer-Verlag London Ltd., part of Springer Nature 2019

Abstract

A green manufacturing technology named “electrostatic minimum quantity lubrication (EMQL)” with water-based Al₂O₃ nanoparticle fluids as cutting fluids was developed in order to improve the cutting property and minimize oil mist concentration during the machining process. The capillary penetration mechanism, oil mist concentration, and heat transfer property of Al₂O₃ fluid EMQL were investigated. The cutting performance of Al₂O₃ fluid EMQL and traditional minimum quantity lubrication (MQL) was compared. The results showed that EMQL could improve the penetrability and heat transfer capacity of the lubricant effectively. Compared with Al₂O₃ fluid MQL and oil-based MQL, Al₂O₃ fluid EMQL reduced oil mist concentration and cutting temperature remarkably and showed similar cutting performances compared with the oil-based MQL. The excellent performance of this water-based Al₂O₃ fluid EMQL technology was mainly due to that EMQL could promote a further penetration of the charged Al₂O₃ nanofluid droplets into the cutting region, which thus reduced the friction force, and the tool durability was maintained obviously and finally presented better machining performance.

Keywords Nanofluid · Electrostatic minimum quantity lubrication · Penetration mechanism · Oil mist concentration · Machining performance

1 Introduction

Mineral cutting fluids have widely been employed to minimize friction and heat at the cutting interface during the manufacturing processes. Nevertheless, it has been demonstrated that the use of mineral fluids might cause negative impacts, such as environmental pollution and operators’ health concerns [1, 2]. To solve these issues, many researchers have made efforts in the last few decades to search for effective alternatives to minimize the use of these mineral fluids [3, 4].

Minimum quantity lubrication (MQL) is one of the promising alternatives, which has attracted wide attention from academia and industry in recent years [5, 6]. In MQL machining,

biodegradable oils are generally atomized with compressed air and form oil mists, which are then fed into the machining zone with a small flow rate of 5~200 mL/h for lubrication and cooling. Some studies [7, 8] have confirmed that the oil-based MQL technologies could effectively enhance the tool life and improve the processing quality. However, good results with the oil-based MQL were not always achieved to all types of machining. In general, the cooling involved in oil-based MQL was mainly realized by evaporation of the micro-droplets and convection of compressed air. These therefore were not able to effectively reduce the cutting temperatures, which showed inadequate cooling performance in cutting difficult-to-process materials [9, 10]. For instance, Leppert [11] investigated the turning performance of the oil-based MQL using AISI 316L stainless steel as the workpiece. The results showed that the cutting force and tool wear of this oil-based MQL were larger than those of the wet and dry cutting owing its insufficient cooling performance. Furthermore, since the oil mists of biodegradable oils are used in MQL to lubricate and cool the cutting interface, there will be a large number of oil droplets floating in the working spaces. These oil mists may be contaminated by harmful dust,

✉ Xiaodong Hu
hooxoodoo@zjut.edu.cn

¹ Key Laboratory of Special Purpose Equipment and Advanced Manufacturing Technology, Ministry of Education & Zhejiang Province, Zhejiang University of Technology, 288, Liuhe Road, Zhejiang 310023, Hangzhou, China

microorganisms, and bacteria in the machining environment, which would cause potential hazards to the operator's health [12, 13]. As a result, oil mist separators or electrostatic filters are installed on machine tools in order to reduce the oil mist concentration. Although the oil mist separators can relatively lower the oil mist concentration, it is still higher than the standard value issued by the National Institute for Occupational Safety and Health (NOISH, $PM_{10} \leq 5 \text{ mg/m}^3$, $PM_{2.5} \leq 0.5 \text{ mg/m}^3$) [14, 15]. The electrostatic filters can meet the needs, but the cost of these devices is high owing to their high failure rate and large filter material consumption [16].

Nevertheless, recent studies [17–19] have pointed out that an effective method of reducing cutting temperature and oil mist concentration involved in MQL machining is to employ water-based lubricants as cutting fluids. However, the amount of the lubricants used in MQL is less, which therefore limits the application of the water-based MQL owing to its low viscosity and lubricity [18]. To improve the lubricating ability of water-based lubricant, some researchers proposed that the nano-additives, such as Al_2O_3 , TiO_2 , and MoS_2 , could increase its lubricity, which thus improved its machining performance. For example, Setti et al. [20] comparatively investigated the lubrication performance of water-based Al_2O_3 and CuO fluid MQLs when grinding of Ti–6Al–4 V. They indicated that the cutting temperatures and forces of these nanofluid MQLs were much lower than those of the baseline MQL. Najiha and Rahman [21] investigated the cutting performance of water-based TiO_2 fluid MQL when milling of aluminum alloy. They reported that TiO_2 fluid MQL presented higher tool life and better cooling performance compared with those of the baseline MQL. Zhang et al. [22] and Yang et al. [23] investigated the machining performance of the conventional MQL and MoS_2 fluid MQL, comparatively. They found that MoS_2 fluid MQL presented a higher material removal rate and lower cutting force compared with those of the baseline MQL. Despite the remarkably improved performance with the addition of nanoparticles, the lubrication capacity of water-based MQL is still much lower than an oil-based MQL, therefore, followed by relatively higher surface roughness and tool wear [24].

In this study, a novel green lubrication technique named “electrostatic minimum quantity lubrication” (EMQL) was proposed to further improve the lubrication ability of water-based nanofluid MQL. EMQL combined the technical advantages of electrostatic spraying (ES) and MQL, which could significantly promote the wettability and penetrability of lubricant droplets in the cutting area and showed better lubricating and cutting performance in comparison with MQL mode [25–27]. For instance, Huang et al. [25] investigated that biodegradable oil lubricant EMQL considerably lowered the friction and wear on the rubbing surface, and the consumption of cutting fluids under EMQL condition was much lower than that of traditional MQL technology. Xu et al. [28]

comparatively studied the MQL and EMQL milling performance using stainless steel as workpiece; they found that the tool wear and roughness value of EMQL were about 30% and 20% lower than those of MQL, respectively. Huang et al. [29] also demonstrated that EMQL could reduce the cutting temperature by 8% in comparison with MQL machining. Furthermore, EMQL technology could also improve the deposition and adsorption properties of lubricant droplets during the machining [30, 31]. Therefore, it is expected that the application of water-based nanofluid EMQL would not only achieve a superior machining performance but also reduce the quantity of the floating oil droplets. However, the penetration mechanism and oil mist concentration of EMQL using water-based nanofluids as cutting fluids have not been researched in the previous studies.

The capillary penetration mechanism, deposition property, and heat transfer capacity of EMQL technology which employed water-based Al_2O_3 nanofluids as cutting fluids were firstly researched. Subsequently, the oil mist concentrations of Al_2O_3 fluid EMQL and traditional MQL were comparatively tested. The machining performance, such as cutting temperature, tool wear, cutting force, and surface quality of the workpiece, using Al_2O_3 fluid EMQL, was systematically verified under appropriate parameters. Finally, the lubricating mechanism of the Al_2O_3 fluid EMQL was revealed through a tribological analysis. The cutting performance using Al_2O_3 fluid MQL and LB-2000 vegetable oil lubricant MQL was also investigated to present the baseline. The LB-2000 vegetable oil is widely used in the MQL process and has advantages of non-toxic and biodegradable [32]. It is believed that this environmentally friendly technology could be a beneficial substitution for the conventional vegetable oil lubricant MQL.

2 Experimental details

2.1 Water-based Al_2O_3 nanofluids

Al_2O_3 nanoparticles of 40 nm in diameter were used as additives in this study, which are commercially available. Hexadecyl trimethyl ammonium bromide (CTAB) and polyethylene glycol 300 (PEG 300) were used as surfactant and tackifier, respectively. To prepare water-based Al_2O_3 nanofluids, PEG 300 was dispersed into the purified water firstly with mass fraction of 60 wt% at ambient temperature. Subsequently, Al_2O_3 nanoparticles were added to the prepared water PEG solution with mass ratios of 0.1 wt%, 0.5 wt%, 1.0 wt%, 1.5 wt%, 2.0 wt%, and 2.5 wt% [20, 33]. CTAB was simultaneously added into these Al_2O_3 suspensions at a concentration of 0.5 wt%. Subsequently, the suspensions were ultrasonically de-agglomerated using an ultrasonic probe (Chenggong Ultrasonic Equipment Co., Ltd., China) for 1 h. During ultrasonic dispersion process, the suspension

temperature needs to keep constant using a chilling water bath. Finally, as can be seen from Fig. 1 that the prepared water-based Al_2O_3 nanofluids after 30 days of static storage were still considerably stable without precipitation and stratification.

2.2 EMQL device

Figure 2 shows the schematic diagram of EMQL milling system. As seen, the lubrication equipment mainly consists of an electrostatic power supply (EST705, output-voltage of 0 to approximately -40 kV, Beijing Huajinghui Technology Ltd., China), an air source processor, and a precision oil supply peristaltic pump. With EMQL system, the oil pipe in the charging device was embedded with an electrode, the lubricants were electrostatically charged via this electrode, and the charged oil mists were formed by the compressed air. These charged oil mists were then directly sprayed into the cutting area.

2.3 Deposition property tests

In general, MQL machining will achieve a low concentration of oil mists in workshops, if oil droplets produced in the process can sufficiently deposit onto the surfaces of workpieces and worktable, i.e., a high-deposition quantity. Figure 3 shows the schematic diagram of a device used for evaluating the deposition performance of oil droplets under different lubrication conditions. The vertical distance between horizontally fixed nozzle and fixture was 60 mm (the nozzle was about 60 mm away from the worktable during the machining experiment), and the horizontal distance between nozzle and collecting sheets was 100–1500 mm (the horizontal distance between the nozzle and side wall of machine tool was 1550 mm). The material of these collecting square sheets was AISI-304 stainless steel with 16 cm^2 in the area (A). The testing air pressure and flow rate of MQL/EMQL were 0.3 MPa and 20 mL/h, respectively. The collection time was 30 min. The deposited droplet weights (M) were measured using an electronic analytical balance. The formula M/A was then figured out to present the deposition weight on per unit

area of different lubrication conditions. Before testing, all the collecting sheets were immersed in acetone and cleaned by ultrasound for 10 min to remove surface impurities. All tests were performed three times in parallel and reported the average values.

2.4 Oil mist concentration tests

The oil mist quantity of different lubrication mode in the milling machine was measured using 8 stages aerosol cascade sampler. The sampler was placed inside the milling machine with the distances of 0.5 m from the spindle and 1.5 m from the ground, as seen in Fig. 4. The sampling flow was 30 L/min, and the acquisition time was 1.5 h. The humidity, temperature, and ambient pressure were measured as the benchmarks before testing, and the milling center was ventilated for 1 h after each test to obtain a constant testing context. Table 1 lists the milling conditions, and every test was performed three times and recorded the average values. The following equations [34] were then calculated to obtain the concentration of the PM 10 and PM 2.5:

$$C = 1000 \times (W_1 - W_2) / V_0 - C_0 \quad (1)$$

$$V_0 = q_v \times t \frac{273}{273 + K} \frac{P_0}{101324.72} \quad (2)$$

where C is the resulting oil mist concentration (mg/m^3), C_0 is the oil mist concentration inside the milling center before testing (mg/m^3), W_1 is the filter membrane weight after testing (mg), W_2 is the filter membrane weight before testing (mg), V_0 is the air volume with standard conditions (L), t is the testing duration (s), q_v is the sampling flow (L/min), K is the room temperature ($^\circ\text{C}$), and P_0 is the atmospheric pressure (MPa).

2.5 Heat transfer tests

The cooling performance of Al_2O_3 fluid EMQL was measured under a steady-state condition using a heat transfer testing device, as shown in Fig. 5. The heating sheet of $10\text{ mm} \times 3\text{ mm} \times 0.2\text{ mm}$ in dimension and made of Ni-Cr alloy was

Fig. 1 Water-based Al_2O_3 nanofluids after 30 days of static storage: **a** 0.1 wt% Al_2O_3 lubricant, **b** 0.5 wt% Al_2O_3 lubricant, **c** 1.0 wt% Al_2O_3 lubricant, **d** 1.5 wt% Al_2O_3 lubricant, **e** 2.0 wt% Al_2O_3 lubricant, and **f** 2.5 wt% Al_2O_3 lubricant

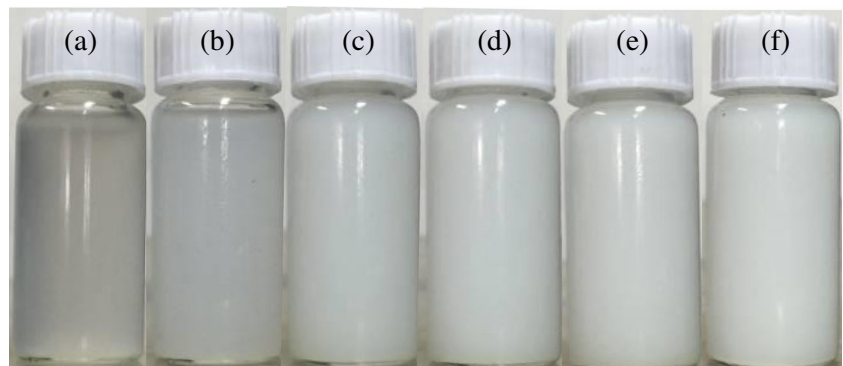
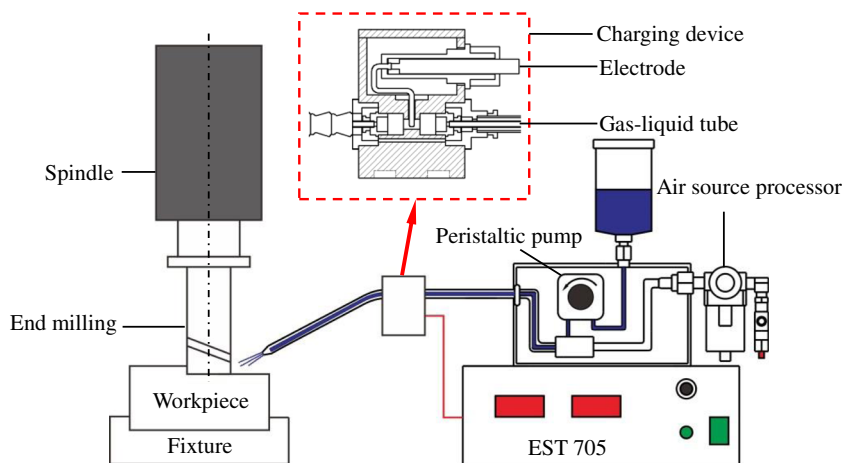


Fig. 2 Structure diagram of EMQL milling system



heated using low voltage and high alternating current. A Cu-Ni thermocouple (TT-J-30) connected a thermos detector (RX4006D, Hangzhou Control Automation Technology Co., Ltd., China) was welded onto the surface of the heating sheet to online monitor and its surface temperatures. The measurement was performed as follows: the sheet was first heated to a specified temperature (T_w). The EMQL system was then turned on to cool the sheet. As the sheet temperature reached a constant value, the voltage (U) and current (I) of the heating sheet were recorded. Subsequently, the heat flux density (Q) could be determined using the equation, $Q = UI/A$, where A is the heat transfer area (0.3 cm^2). Finally, the heat transfer coefficient (h) could be obtained through the equation, $h = Q/(T_w - T_f)$ [35], where T_f is the temperature of the lubricant droplets. All tests were performed three times in parallel and calculated the average values.

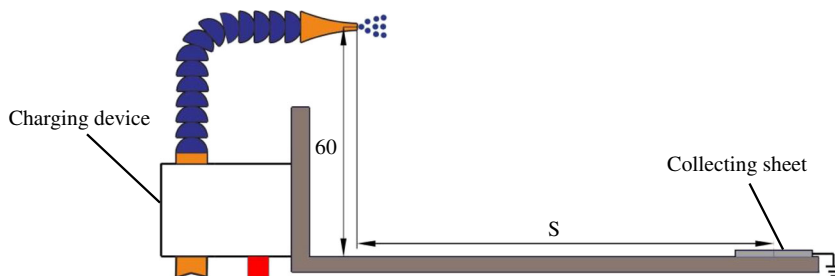
2.6 Milling tests

The EMQL machining tests using water-based Al_2O_3 nanofluids as cutting fluids were performed on a VDF-850 milling center (DMGT, China). Figure 6 shows the physical picture of this milling experimental device. The tested workpiece material was AISI 304 stainless steel, which had dimensions of $210 \text{ mm} \times 105 \text{ mm} \times 130 \text{ mm}$ and $20 \text{ mm} \times 20 \text{ mm} \times 100 \text{ mm}$. The bigger one was used to measure the surface roughness, tool wear, and cutting force. The smaller one was employed for testing the machining temperatures. Before

testing, all workpieces were pre-cut 2 mm to ensure the consistent surface properties under all machining experiments. The cemented carbide insert coated with TiW (Sumitomo, Rineck, APMT160408PDER-H08) was employed as a cutting tool. A 35-mm diameter milling cutter was used during the machining process. The insert was replaced after each experiment to ensure the same experimental condition. The tool manufacture's recommendation was consulted to select appropriate feed rate and cutting speed. During the machining process, the workpiece and machine tool were both grounded to keep a neutral property under all lubrication environments. Table 1 shows the test conditions.

The maximum flank wear of the cutting tools under different lubrications was measured using a microscope (VW-6000, Kean, Japan). The worn tools were analyzed using a scanning electron microscopy (EVO18, Zeiss, Germany) to study the wear mechanisms. The 9129A Kistler dynamometer was employed to record the cutting forces under different lubrication conditions. The equation, $F_R = (F_x^2 + F_y^2 + F_z^2)^{1/2}$, was used to calculate the resulting cutting force (F_R). A roughness measuring instrument (SJ-210, Mitutoyo, Japan) was performed to measure the roughness value (R_a) of the workpiece surface after all testing conditions. The thermocouple (TT-J-30) connected with the thermodetector (RX4006D) was placed into the workpieces to measure the machining temperatures. The distance between the measuring point of the thermocouple and the machining surface was 2 mm. It should be noted that the measured temperatures achieved using the

Fig. 3 Schematic diagram of a deposition testing device



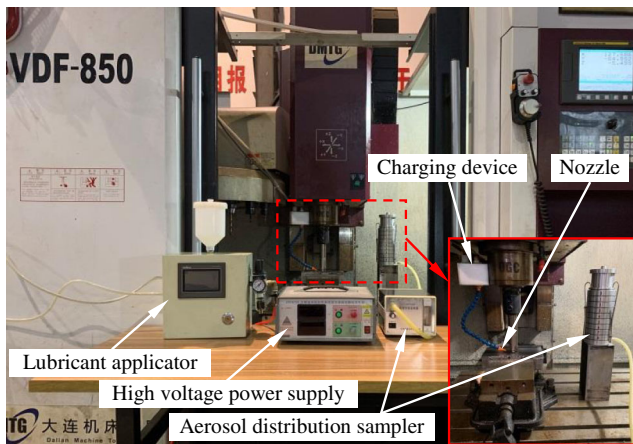


Fig. 4 Photographic view of the oil mist concentration experimental setup

above method were not the true machining temperatures; the purpose of these tests was to compare the cooling performance of the different lubrication conditions. Every test was performed three times and calculated the average result.

2.7 Tribological tests

To reveal the lubricating mechanism of the EMQL technology, the wear characteristics of the Al_2O_3 fluid EMQL were investigated on the MMW-1 multifunctional tribometer using ball-on-disk friction pairs, as shown in Fig. 7. The material of the testing balls (59–61 HRC, $\Phi = 12.7$ mm) was AISI-52100. The testing disks (25–28 HRC) were made of AISI-52100 and were 1 mm in thickness and 32 mm in diameter. The samples were grounded. All tests were conducted in ambient condition

Table 1 Milling conditions

Machine	VDF – 850 vertical milling center, China
Workpiece material	AISI-304 stainless steel Dimension 210 mm × 105 mm × 110 mm and 20 mm × 20 mm × 100 mm block
Cutting tool	TAP400R C32-35-200L, Juhai tools, China Diameter 35 mm, three teeth
Inserts	APMT1604PDER-H08, Sumitomo Coated cemented carbide
Cutting parameters	Cutting speed 100 m/min Feed rate 0.1 mm/tooth Axial depth of cut 1 mm Radial depth 5 mm Single cutting length 210 mm
Lubricants	Oil lubricant: Accu-Lube 2000; Water-based lubricant: water PEG solution Water-based Al_2O_3 fluids
MQL/EMQL supply	Charging voltage – 4 kV Oil flow rate 20 mL/h Air pressure 0.3 MPa Nozzle position 45° toward the flank face Nozzle distance 20 mm

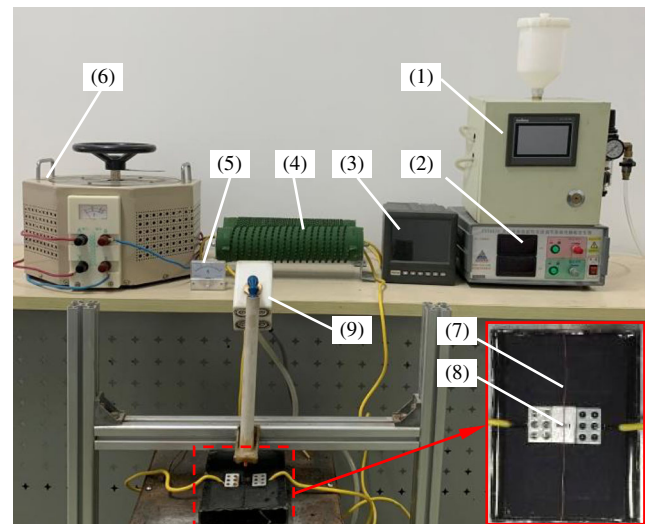


Fig. 5 Steady-state heat transfer test device: (1) precision lubricant applicator, (2) high-voltage electrostatic power supply, (3) thermodetector, (4) power transformers, (5) ammeter, (6) voltage regulator, (7) thermocouple, (8) Ni-Cr alloy heating sheet, (9) charging device

at the charging voltage of – 4 kV, flow rate of 20 mL/h, air pressure of 0.3 MPa, rotational speed of 1200 r/min, and applied load of 294 N. Testing time was 10 min. All the balls and disks were immersed in acetone and cleaned by ultrasound for 10 min before and after testing, and the wear surface on the disks was evaluated by SEM. The elemental mapping was performed by use of the energy dispersive X-ray spectroscopy (EDS) analysis.

3 Results and discussion

3.1 Penetration mechanism of EMQL

The lubrication performance of MQL, such as the wettability and penetrability of the lubricant droplets, is generally

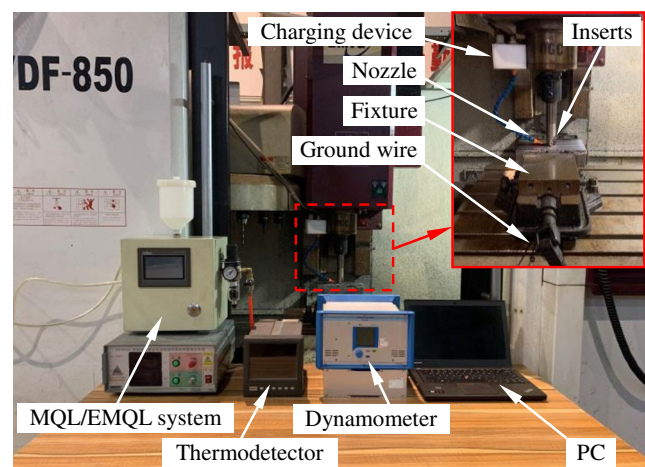


Fig. 6 Physical picture of milling experimental device

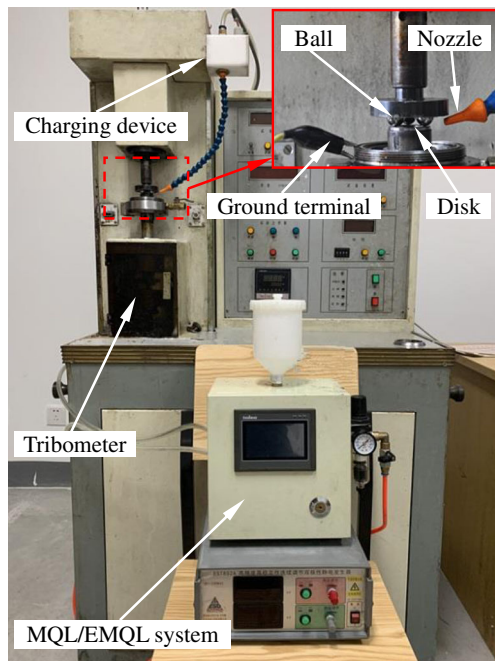


Fig. 7 Photographic view of the tribological testing configuration

evaluated by their contact angle and surface tension. In the previous studies, EMQL was found to reduce the contact angle and surface tension of the droplets remarkably, in comparison with MQL (0 kV), which could present better wetting ability and penetration performance. Such reductions might be attributed to the fact that the electrostatic charges adsorbed on the surface of the droplets were mutually exclusive, which could produce an electrostatic force that was opposite to the surface tension and thus reduced its contact angle and surface tension. The relation between surface tension and the droplet charge quantity could be well understood using the following empirical equation [36].

$$\sigma = \sigma_0 - \frac{q^2}{8\pi^2\epsilon_0 d^3} \tag{3}$$

where σ is the charged droplet surface tension, σ_0 is the neutral droplet surface tension, q is the charge quantity of the droplet, ϵ_0 is vacuum permittivity, and d is droplet diameter. As seen in Eq. (3), when the charging voltage was enhanced, the charge quantity (q) will be increased, which thus resulted in a rapid reduction in the surface tension.

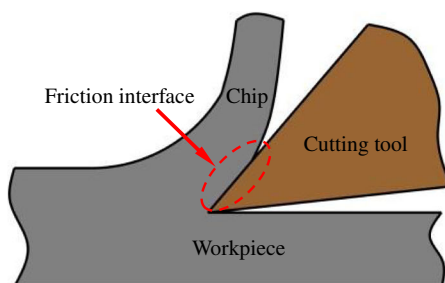


Fig. 8 Capillary penetration model of the lubricants

Table 2 Surface tension and contact angle versus charging voltage

Voltage/kV	Surface tension $\gamma/\text{N m}^{-1}$	Contact angle $\theta/^\circ$
0	0.055	70
-2	0.053	64
-4	0.051	58
-6	0.043	52
-8	0.036	48
-10	0.024	38

To well understand the capillary penetration mechanism of the charged lubricants, the kinetic process of capillary penetration was studied. To facilitate the analysis of the capillary penetration process, the following assumptions were made for the capillary in the tool-chip interface.

1. A large number of capillary tubes were distributed between the tool-chip contact area and were arranged along the direction of the chip flow.
2. A single capillary was a cylinder with an opening at one end, closed at another end, and the interior was a vacuum. The capillary length was about 1/3~2/3 of the tool-chip contact length, with a radius of 0.1–100 μm . According to Godlevski et al. [37], the capillary radius could be assumed as 0.5 μm .

Figure 8 shows the capillary penetration model of the lubricant. The penetration process was mainly affected by three forces: capillary force (F_{cap}), atmospheric pressure (F_p), and viscosity resistance between the lubricant and capillary wall (F_{visco}).

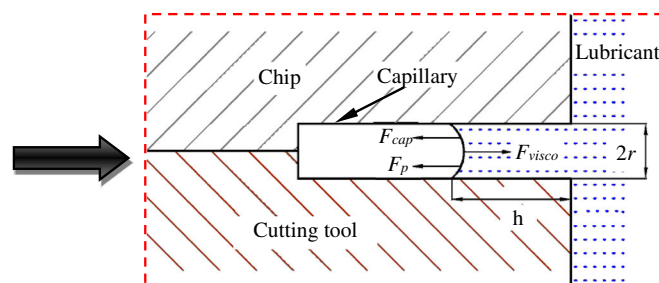
According to the Young-Laplace equation [38], the driving pressure in the capillary can be written as follows:

$$\Delta P = 2\gamma\cos\theta/r \tag{4}$$

The total capillary force is

$$F_{\text{cap}} = \Delta P \cdot \pi r^2 = 2\pi r\gamma\cos\theta \tag{5}$$

Here, r is the capillary radius and was assumed as 0.5 μm ; γ and θ are lubricant surface tension and contact angle, respectively.



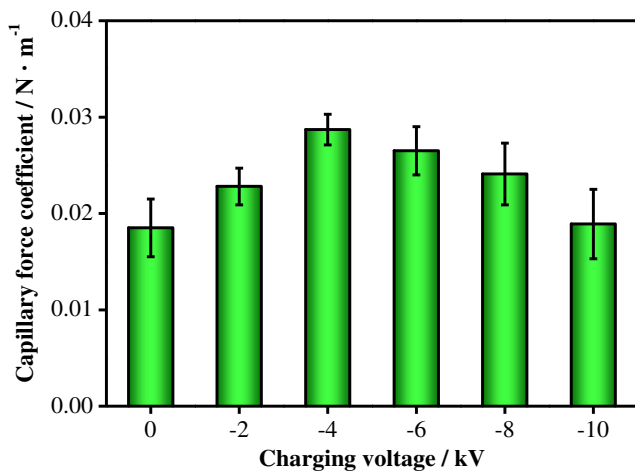


Fig. 9 Variation of the capillary force coefficient under different charging voltage

The viscous resistance can be obtained from the law of the internal friction of Newton viscous fluid and the Hagen-Poiseuille equation [39]:

$$F_{\text{visco}} = 2\pi rh \cdot \tau \tag{6}$$

h is the penetration depth; τ is the viscous frictional shear force.

$$\tau = \eta \cdot \frac{4\bar{v}}{r} \tag{7}$$

η is the dynamic viscosity of the lubricant; \bar{v} is the average velocity of the lubricant penetration.

$$\bar{v} = \frac{dh}{dt} \tag{8}$$

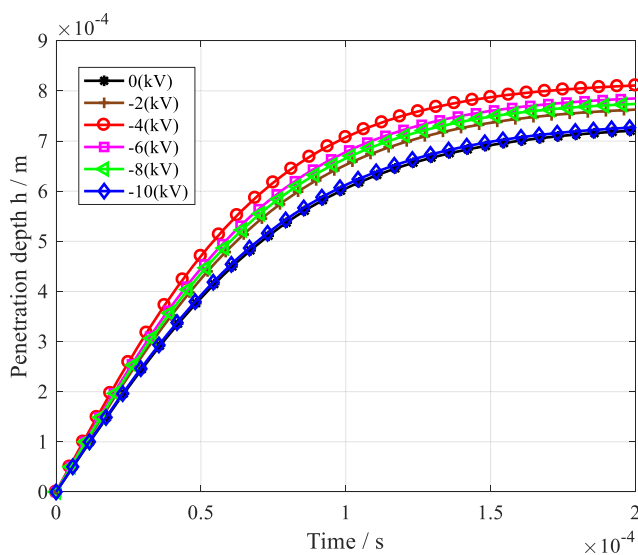


Fig. 10 Variation of lubricant penetration depth under different charging voltage

Atmospheric pressure can be obtained as

$$F_p = \pi r^2 \cdot P_{\text{atm}} \tag{9}$$

P_{atm} is the standard atmospheric pressure, $P_{\text{atm}} = 1.01 \times 10^5 \text{ N/m}^2$.

According to the momentum theorem, the inertia force of the lubricant during the penetration process can be written as

$$\frac{d(m\bar{v})}{dt} = F \tag{10}$$

Here, m is the penetration quality of the lubricant, F is the resultant force of F_{cap} , F_p , and F_{visco}

$$F = F_{\text{cap}} + F_p - F_{\text{visco}} \tag{11}$$

As discussed above, the capillary dynamic equation can be written as

$$2\pi r \gamma \cos\theta + \pi r^2 \cdot P_{\text{atm}} - 8\pi \eta h \bar{v} = \frac{d(m\bar{v})}{dt} \tag{12}$$

During the penetration process, F_{cap} was the main capillary driving force. Under the same capillary size, the capillary force was related to the contact angle and surface tension. Defining the capillary force coefficient, C :

$$C = \gamma \cdot \cos\theta \tag{13}$$

Table 2 lists the values of contact angle and surface tension of Al_2O_3 fluids, plotted as a function of voltage. The measuring methods of contact angle and surface tension were well introduced in [25].

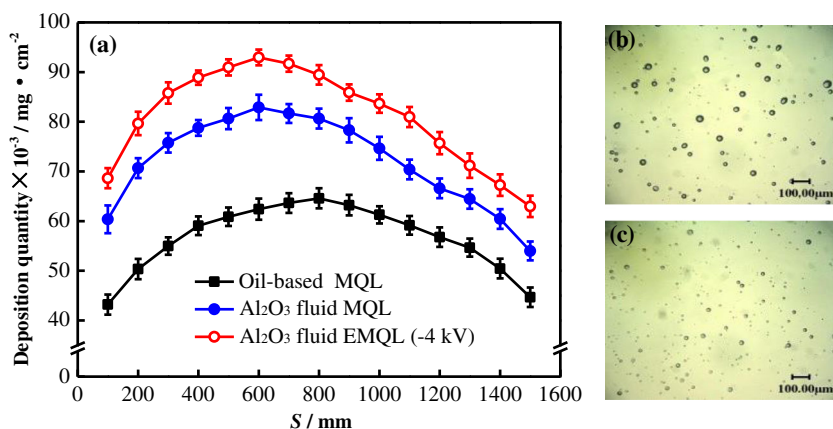
According to Table 2, the variation of the capillary force coefficient under different charging voltage is shown in Fig. 9. The highest capillary force coefficient was achieved when the voltage was -4 kV , with its value being 35.5% higher than that of 0 kV , indicating a higher capillary force during the penetration process. However, a further increase in voltage led to a decrease in the capillary force coefficient. Higher voltage presented lower surface tension, which would degrade the capillary force.

During the penetration process, the charge in the lubricant will be continuously lost, so the charge loss time of the cutting fluid should be considered. According to Gauss theorem [40], the charge loss time constant can be written as

$$K = \frac{\epsilon_o \epsilon_R}{R} \tag{14}$$

Here, ϵ_o is the vacuum permittivity, and $\epsilon_o = 8.85 \times 10^{-12} \text{ F/m}$; ϵ_R is the permittivity of the lubricant, $\epsilon_R = 30.6 \text{ F/m}$; R is the electrical conductivity of the lubricant, $R = 1.5 \times 10^{-5} \text{ s/m}$. It is generally believed that all charges in the lubricant are lost when the charge loss time was 3 K . As

Fig. 11 a Deposition quantity of the lubricant droplets under different lubrication conditions and lubricant droplet size under b Al₂O₃ fluid MQL and c oil-based MQL (flow rate 20 mL/h, air pressure 0.3 MPa)



discussed above, the charge loss time of Al₂O₃ lubricant was 0.54×10^{-4} s.

Using Matlab to solve the capillary dynamic equation (Eq. 12), Fig. 10 shows the variation of penetration depth under the influence of charging voltage. It is seen that -4 kV EMQL presented highest penetration depth during the whole penetration process, with its value being 20.1% higher than that of MQL mode (0 kV) when the penetration time was 0.54×10^{-4} s. This calculation result proved that EMQL could promote more lubricant penetrating into the tool-chip interface under appropriate voltage, and more lubricant could take part in the lubrication process and thus improved its lubrication performance.

3.2 Deposition property

Figure 11a shows the deposition quantity of lubricant droplets under oil-based MQL, 1 wt% Al₂O₃ fluid MQL, and EMQL. It is seen that Al₂O₃ fluid MQL achieved a larger deposition

quantity than oil-based MQL at all tested distances. The highest deposition quantity of Al₂O₃ fluid MQL was observed when $S = 600$ mm, and its value was 32.9% larger in comparison with oil-based MQL, indicating better deposition property. The Al₂O₃ nanofluid contained 60 wt% PEG 300, which belongs to a kind of high molecular weight polymer. The Al₂O₃ nanofluid showed higher extensional viscosity owing to the addition of this high molecular polymer, which presented larger elasticoviscosity, and the lubricant was not easy to break and so that the droplet size was relatively large, as seen in Fig. 11 b and c, thus presenting higher deposition quantity [41, 42]. As shown in Fig. 11a, the deposition quantities of Al₂O₃ fluid EMQL were much higher in comparison with Al₂O₃ fluid MQL. With EMQL, an induced electrostatic field was generated between the grounded collecting sheets and charged droplets, in which the charged droplets would be deposited onto these sheets more effectively driven by the electrostatic force and hence resulted in a high-deposition quantity.

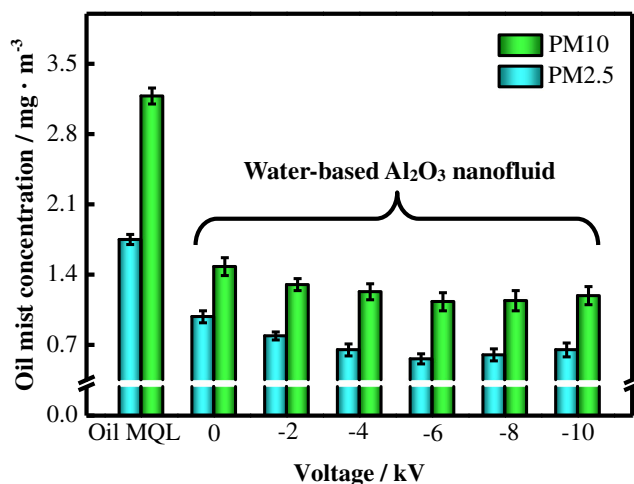


Fig. 12 Effect of charging voltage on oil mist concentration under different lubrication conditions (flow rate 20 mL/h, air pressure 0.3 MPa, cutting speed 100 m/min, feed rate 0.1 mm/tooth, axial depth of cut 1 mm, radial depth 5 mm, nozzle position 45° toward the flank face, nozzle distance 20 mm, testing duration 1.5 h)

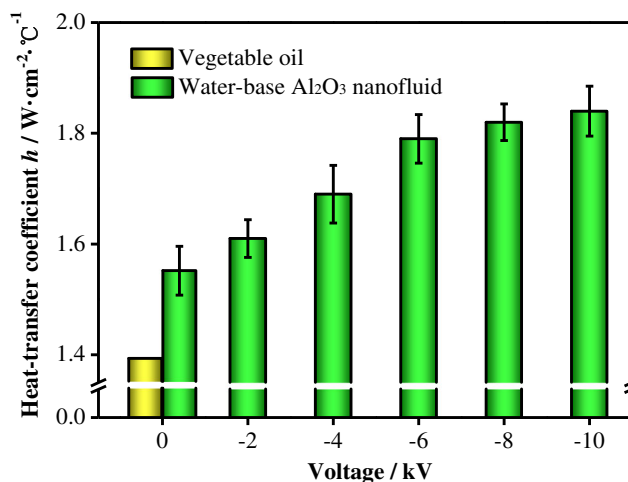


Fig. 13 Heat transfer coefficient of MQL and EMQL lubrication modes (flow rate 20 mL/h, air pressure 0.3 MPa)

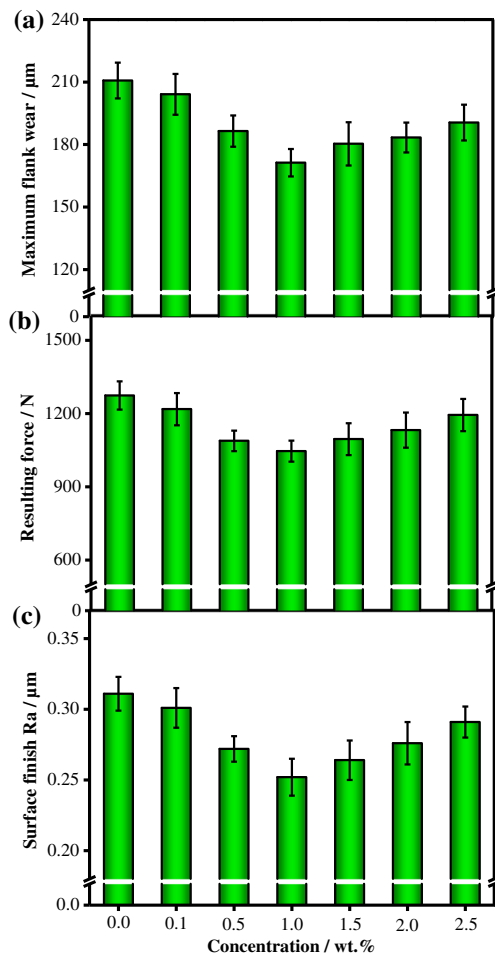


Fig. 14 Effect of Al_2O_3 concentration on **a** tool wear, **b** cutting force, and **c** surface finish under Al_2O_3 fluid MQL (flow rate 20 mL/h, air pressure 0.3 MPa, cutting speed 100 m/min, feed rate 0.1 mm/tooth, axial depth of cut 1 mm, radial depth 5 mm, nozzle position 45° toward the flank face, nozzle distance 20 mm, cutting length 2100 mm)

3.3 Oil mist concentration

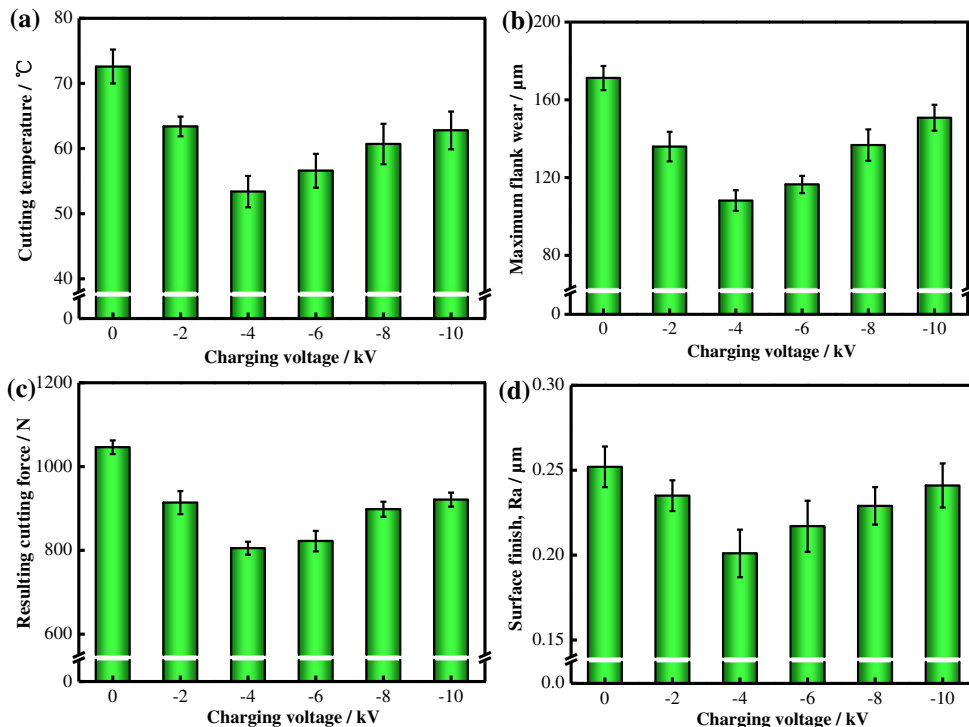
The variation of the oil mist concentration using oil-based MQL, 1 wt% Al_2O_3 fluid MQL, and EMQL is shown in Fig. 12. It is seen that the water-based Al_2O_3 fluid MQL presented much lower PM 10 and PM 2.5 concentration values compared with oil-based MQL; the respective reductions of 56.6% and 44% were achieved, indicating a better oil mist suppression ability. This is because that the addition of PEG 300 promoted more water-based nanofluid droplets depositing on the surface of machine tool and workpiece, which therefore reduced the oil mist content in the machining environment and thus presented lower oil mist concentration. Furthermore, the water-based droplets floating in the machining environment were more easily evaporated in comparison with oil droplets, which reduced the number of droplets effectively and thus presented better environment quantity.

As seen in Fig. 12, the PM 10 and PM 2.5 concentrations produced with Al_2O_3 fluid EMQL were much lower than those of the Al_2O_3 fluid MQL; the lowest concentration values were achieved when the voltage was -6 kV, which resulted in a PM 10 reduction of 20.3% and a PM 2.5 reduction of 42.9% compared with Al_2O_3 fluid MQL, suggesting the improved environmental quality. Particularly, it should be noted that the lowest concentration values of PM 10 and PM 2.5 achieved with Al_2O_3 fluid EMQL were 1.13 mg/m^3 and 0.56 mg/m^3 , respectively, close to the standard values ($\text{PM 10} \leq 5 \text{ mg/m}^3$, $\text{PM 2.5} \leq 0.5 \text{ mg/m}^3$) issued by the National Institute for Occupational Safety and Health (NOISH) [14]. In EMQL machining, an electrostatic field was induced and generated between the workpiece and charged droplet, which promoted deposition of these charged droplets onto the workpiece and machine tool. Furthermore, the improvement in the wettability and penetrability of the droplets could relatively increase their quantity and usage rate in the cutting region, thus reducing the quantities of droplets floating in the workshop. As seen in Fig. 12, the PM 10 and PM2.5 concentration values showed a slight increase when the charging voltage exceeded -4 kV. This is because a stronger electrostatic repulsion would be formed between the charged droplets under higher voltage conditions, which would cause excessive spray angle. This might make some of the droplets spill out of the cutting region and therefore resulted in an increased oil mist concentration.

3.4 Heat transfer property

The effect of voltage on the heat transfer coefficient (h) using 1.0 wt% Al_2O_3 fluid EMQL is shown in Fig. 13. It should be noted that the “0 kV” in fact refers to 1.0 wt% Al_2O_3 fluid MQL, and the heat transfer result achieved using the oil-based MQL was presented for comparison. The specified temperature in this test was set at 100°C . As seen, the Al_2O_3 fluid EMQL produced higher values of heat transfer coefficient compared with MQL mode at all tested voltages. The highest heat transfer coefficient was obtained using -10 kV Al_2O_3 fluid EMQL, with its value being 18.8% and 30.2% higher than that of the Al_2O_3 fluid MQL and oil-based MQL, respectively. These experimental results proved that EMQL could enhance the heat transfer capacity of MQL and thus improved its cooling performance. This can be attributed to the improved wettability of the charged droplets when EMQL was used, which allowed the droplets to cover the surface of the heating sheet more easily, thus improving the heat transfer efficiency of evaporation of the droplets and led to a better cooling effect.

Fig. 15 Effect of charging voltage on **a** cutting temperature, **b** tool wear, **c** resulting cutting force, and **d** surface finishing under EMQL mode (flow rate 20 mL/h, air pressure 0.3 MPa, cutting speed 100 m/min, feed rate 0.1 mm/tooth, axial depth of cut 1 mm, radial depth 5 mm, nozzle position 45° toward the flank face, nozzle distance 20 mm, cutting length 2100 mm)



3.5 Milling performance

3.5.1 Effect of Al₂O₃ concentrations

The effect of Al₂O₃ concentration on tool wear, cutting force, and surface finish of MQL was investigated and is shown in Fig. 14. The addition of Al₂O₃ improved the machining performance significantly, as seen in Fig. 14. The lowest tool wear, cutting force, and R_a value were achieved from the 1.0 wt% Al₂O₃ fluid MQL, which resulted in a respective

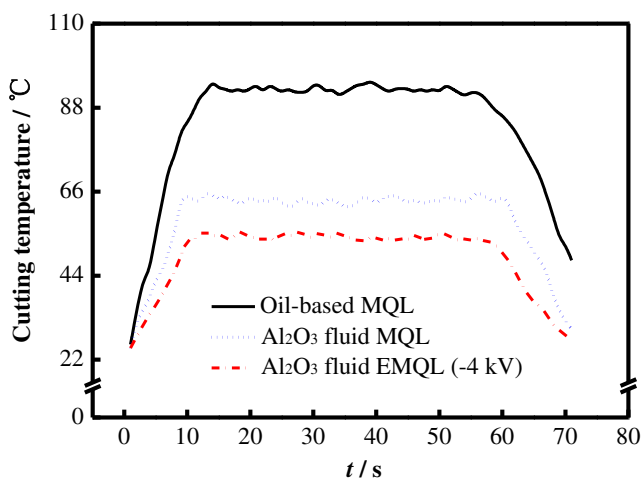


Fig. 16 Measurement signal images of the cutting temperature under different cutting environment (flow rate 20 mL/h, air pressure 0.3 MPa, cutting speed 100 m/min, feed rate 0.1 mm/tooth, axial depth of cut 1 mm, radial depth 5 mm, nozzle position 45° toward the flank face, nozzle distance 20 mm, cutting length 2100 mm)

reduction of 18.7%, 17.9%, and 20% than baseline MQL. Such an improvement in the machining performance might be due to that the spherical Al₂O₃ nanoparticles served as miniature ball bearings to disperse the stress at the tool-chip interface and therefore resulted in lower friction and wear [43]. Also, these Al₂O₃ nanoparticles acted as a medium to fill the grooves and concaves of the rubbing surface, which avoided the direct contact of friction peaks and hence achieved a better surface quality [33]. As seen in Fig. 14, the tool wear, cutting force, and R_a value were increased when the Al₂O₃ concentration was further enhanced. This is because that at a higher concentration, the agglomerations of Al₂O₃ might form on the interface, which were not conducive to the formation of a lubricating film on the cutting interface and thus resulted in a relatively poor milling performance [44]. As presented above, the 1.0 wt% Al₂O₃ fluid MQL produced better milling performances, which was therefore used as a benchmark for subsequent experiments.

3.5.2 Effect of charging voltage

Figure 15a shows the effect of charging voltage on the cutting temperature using 1.0 wt% Al₂O₃ fluid EMQL. When the -4 kV EMQL was used, the lowest cutting temperature was achieved, with its value being 19.1% lower than that of the Al₂O₃ fluid MQL. The result indicated that Al₂O₃ fluid EMQL could reduce the cutting temperature effectively. Due to the improved penetration performance, more Al₂O₃ nanofluid could enter and lubricate the rubbing interface,



Fig. 17 Microscopic images of the flank wear using **a** oil-based MQL, **b** Al_2O_3 fluid MQL, and **c** Al_2O_3 fluid EMQL with -4 kV (flow rate 20 mL/h, air pressure 0.3 MPa, cutting speed 100 m/min, feed rate

0.1 mm/tooth, axial depth of cut 1 mm, radial depth 5 mm, nozzle position 45° toward the flank face, nozzle distance 20 mm, cutting length 2100 mm)

which would reduce the friction-induced heat and consequently presented a lower cutting temperature. In addition, the improved wetting ability by using EMQL could enhance the evaporative heat transfer of the droplets, which would lead to a lower temperature too. However, the cutting temperature was enhanced when the charging voltage was further increased, as seen in Fig. 15a. This is because that lower capillary penetrability was performed using a higher charging voltage, which therefore reduced the content of the lubricant in the cutting interface, thus presenting higher cutting temperature. Moreover, higher voltage might lead to an excessive spray angle [45, 46], which would degrade the droplet distribution on the small cutting region, which therefore reduced the cooling performance relatively.

The effect of charging voltage on the tool wear using Al_2O_3 fluid EMQL is shown in Fig. 15b. It is seen that Al_2O_3 fluid EMQL obtained lower tool wear in comparison with Al_2O_3 fluid MQL under all voltage conditions. As the voltage was rose to -4 kV, the Al_2O_3 fluid EMQL presented the lowest tool wear, which showed up a reduction of 36.8% in comparison with Al_2O_3 fluid MQL. Owing to the improved penetration performance, the charged Al_2O_3 nanofluid could effectively penetrate into the cutting zone, more lubricant took part in the lubrication process, which thus relieved the friction and heat between the tool-chip interface. As a result, the wear resistance and strength of the cutting tool were maintained during the machining and thus decreased the tool wear considerably.

Figure 15c and d show the effect of charging voltage on the cutting force and surface roughness using Al_2O_3 fluid EMQL. As expected, the lowest cutting force and R_a value were observed with the -4 kV Al_2O_3 fluid EMQL, which presented a

respective reduction of 23% and 20.2% compared with those of the Al_2O_3 fluid MQL. Due to the better cooling-lubrication performance of the charged Al_2O_3 fluid, EMQL reduced the cutting temperature and tool wear obviously, which resulted in lower cutting force and better surface quantity. Furthermore, the better lubrication would lead to easier slip of chips over the tool and workpiece surfaces, which could help to alleviate the adhesion wear of the cutting tool, and ultimately showed better workpiece surface quality.

Considering the best machining performance of Al_2O_3 fluid EMQL, the charging voltage with -4 kV was selected as invariant parameters in the subsequent tests.

3.5.3 Effect of lubrication technology

Figure 16 shows the measurement signal images of the cutting temperature using oil-based MQL, 1.0 wt% Al_2O_3 fluid MQL, and -4 kV EMQL. It is seen that both of the water-based Al_2O_3 fluid MQL and EMQL showed up much lower cutting temperature compared with that of the oil-based MQL. When the water-based Al_2O_3 droplets were used, a much higher evaporation coefficient of heat transfer could be presented compared with the oil droplets, thus reducing the cutting temperature significantly. It is also seen that the Al_2O_3 fluid EMQL produced the lowest cutting temperature thanks to the better heat transfer property of the charged Al_2O_3 nanofluid. The mean value of the cutting temperature produced by Al_2O_3 fluid EMQL achieved respective reductions of 43.9% and 15.3% than the oil-based and Al_2O_3 fluid MQLs, confirming its effective cooling performance.

Figure 17 shows the microscopic image of the flank wear under oil-based MQL, Al_2O_3 fluid MQL, and EMQL. The

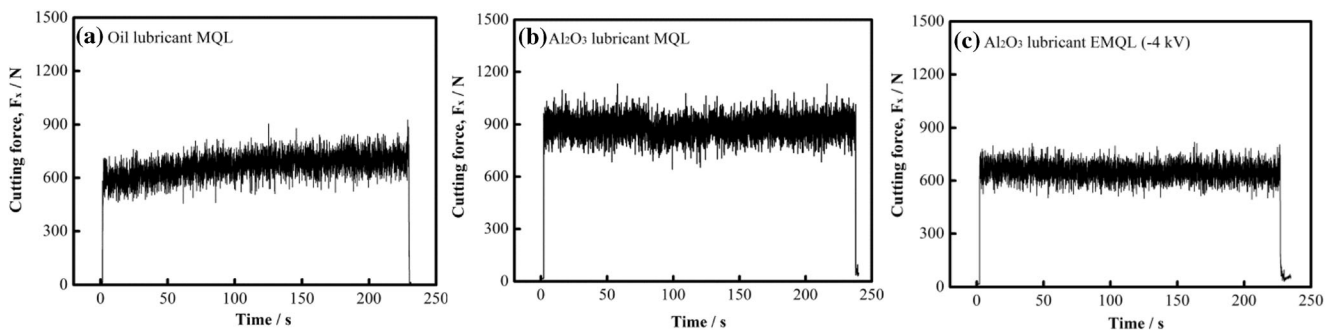


Fig. 18 Measurement signal images of the cutting force (F_x) under different lubrication conditions after the cutting length of 2100 mm (cutting speed 100 m/min, feed rate 0.1 mm/tooth, axial depth of cut 1 mm, radial depth 5 mm)

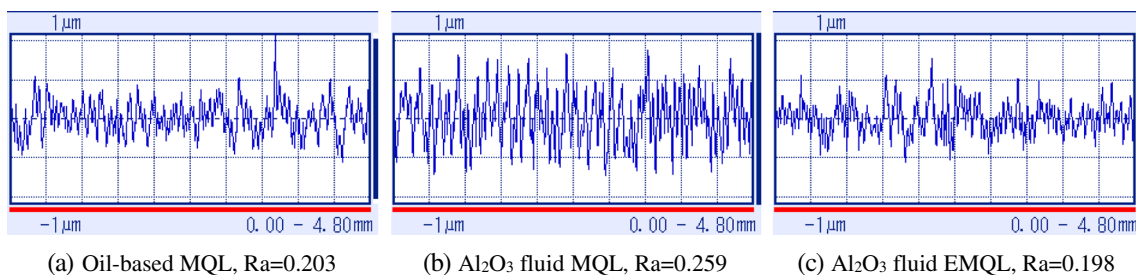


Fig. 19 Surface roughness measurement signal images under different lubrication conditions after the cutting length of 2100 mm (cutting speed 100 m/min, feed rate 0.1 mm/tooth, axial depth of cut 1 mm, radial depth 5 mm)

tested cutting length was 2100 mm. The tool wear of the Al₂O₃ fluid EMQL was lesser than that of the Al₂O₃ fluid MQL under the same testing conditions. Particularly, the Al₂O₃ fluid EMQL produced similar tool wear degree to the oil-based MQL, which suggested the favorable lubricating ability. EMQL altered the physical properties of the droplets, and the charged droplets could lubricate and cool the cutting interface more effectively, thus alleviating the tool wear.

The cutting force (F_x) and surface roughness signal images produced using the oil-based MQL, Al₂O₃ fluid MQL, and Al₂O₃ fluid EMQL are shown in Figs. 18 and 19. As seen, the Al₂O₃ fluid EMQL presented much lower cutting force and

roughness value in comparison with the Al₂O₃ fluid MQL, confirming its effectiveness. Moreover, these results obtained with the Al₂O₃ fluid EMQL were comparable with the oil-based MQL, indicating that the Al₂O₃ fluid EMQL could be an effective alternative to the traditional oil-based MQL.

3.5.4 Tool wear mechanism

Figure 20 shows the SEM images of the tool flank wear produced using the Al₂O₃ fluid MQL and EMQL after 2100 mm cutting length. As seen, the worn flank faces produced from using both lubrication appeared clear adhesion layer and

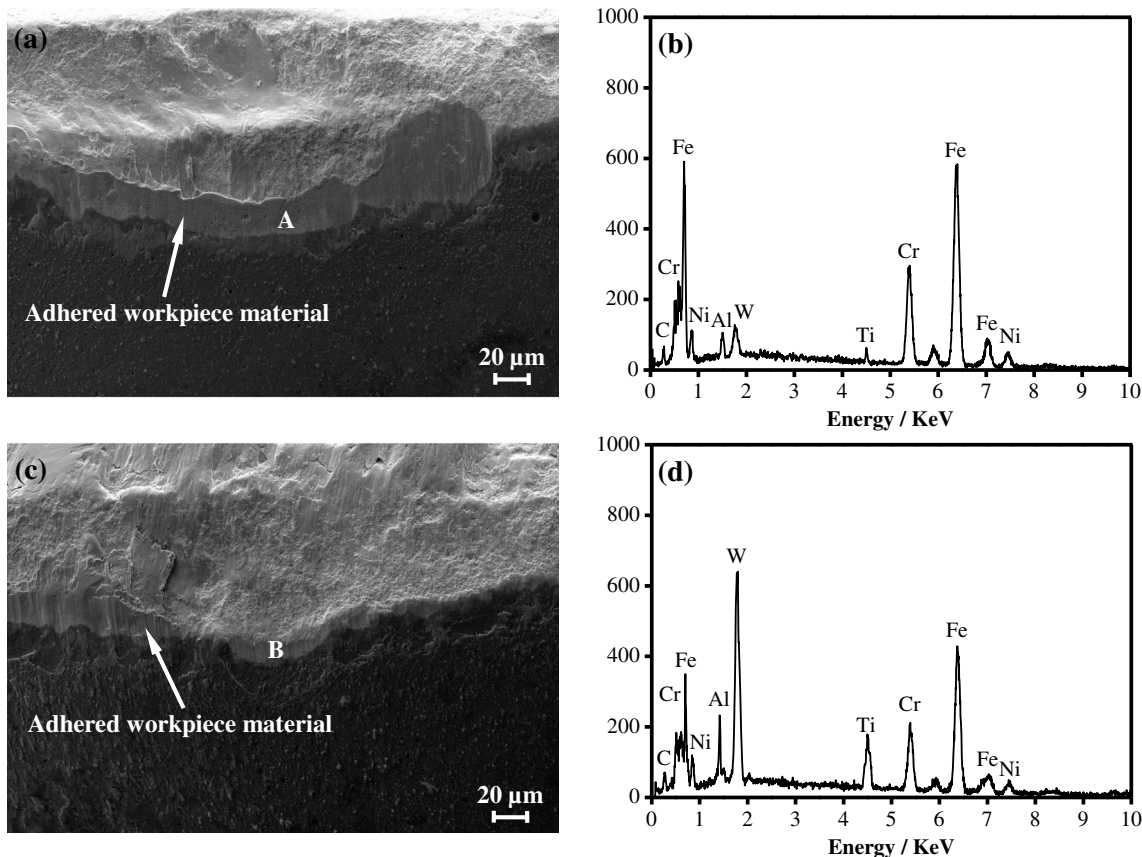
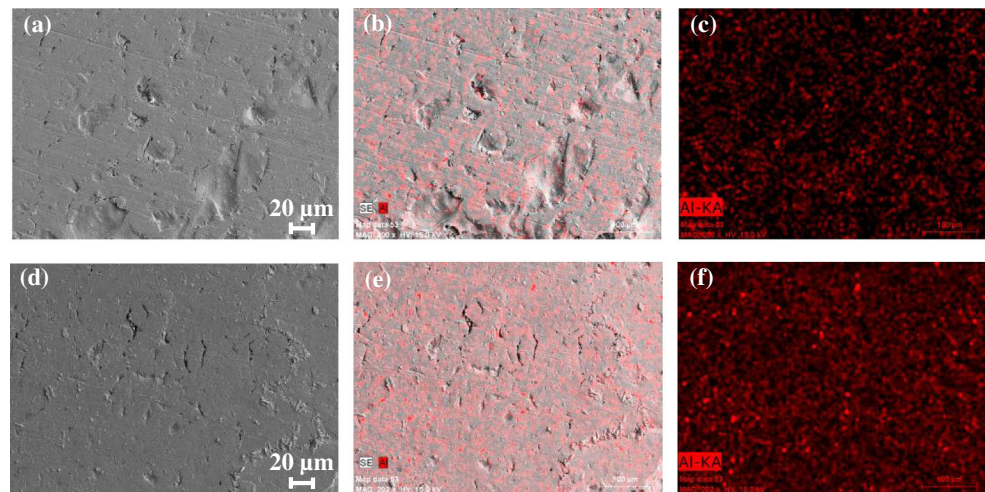


Fig. 20 a SEM micrographs performed on the flank face for Al₂O₃ fluid MQL, b EDS analyses on site A, c SEM micrographs performed on the flank face for Al₂O₃ fluid EMQL with -4 kV, d EDS analyses on site B (flow rate 20 mL/h, air pressure 0.3 MPa, cutting speed 100 m/min, feed

rate 0.1 mm/tooth, axial depth of cut 1 mm, radial depth 5 mm, nozzle position 45° toward the flank face, nozzle distance 20 mm, cutting length 2100 mm)

Fig. 21 SEM electron images of wear mark surface using **a** Al₂O₃ fluid MQL, and **d** Al₂O₃ fluid EMQL with -4 kV; **b** and **c** aluminum mapping on **(a)**; **e** and **f** aluminum mapping on **(d)**



furrows on the rubbing areas, presenting the occurrence of adhesive wear and abrasive wear. During the cutting process, the high cutting temperature was easily produced in the tool-chip contact area, which resulted in the adhesion of chip materials to the cutting edge and thus caused varying extent adhesion wear [47].

The SEM image of the worn cutting edge produced using Al₂O₃ fluid MQL is shown in Fig. 20a, in which an adhesive layer appears on the worn area. The corresponding EDS analysis shown in Fig. 20b detected high concentrations of Fe, Cr, and Ni, indicating serious adhesive wear. This is because that the Al₂O₃ nanofluid droplets produced with MQL technology showed inadequate wettability and penetrability, which could not lubricate the tool-chip interface effectively, thus resulted in severe tool wear.

With the Al₂O₃ fluid EMQL, slight adhesive wear existed on the worn area, as shown in Fig. 20c. This result indicated that the Al₂O₃ fluid EMQL could effectively alleviate the adhesion wear, thus improving the tool durability. The corresponding EDS analysis shown in Fig. 20d detected higher concentrations of W and Ti (the principal chemical elements of tool coating) and a higher concentration of Al, which came from Al₂O₃ nanoparticles, compared with the Al₂O₃ fluid MQL. Due to the improved penetration and wetting capacity, more Al₂O₃ and base lubricant could participate in the lubrication process, which minimized the friction at the cutting area and therefore prolonged the tool life.

3.6 Lubrication mechanism

After tribological testing, the worn surfaces produced using the Al₂O₃ fluid MQL and EMQL were analyzed using SEM and EDS aluminum K α 1 peak mapping and the results are shown in Fig. 21. It is seen that due to the insufficient lubrication, severe scratches and furrows appeared on the worn surface of the disk produced by Al₂O₃ fluid MQL. The corresponding EDS mapping analysis showed in Fig. 21b and c

detected a small amount of aluminum on the worn surface (the red spot in the figures was the detection signal of aluminum). As seen in Fig. 21d, the worn surface produced by Al₂O₃ fluid EMQL was much smoother than that of the Al₂O₃ fluid MQL. The EDS mapping analysis to the worn surface appeared a larger amount of aluminum. These results confirmed the improved penetration performance of the charged Al₂O₃ nanofluid droplets, which increased the amount of Al₂O₃ nanofluid in the friction region, and consequently more Al₂O₃ and base lubricant could take part in the lubrication process and thus presented higher lubrication performance.

4 Conclusions

EMQL machining performance that uses water-based Al₂O₃ nanofluids was systematically researched. The charged Al₂O₃ nanofluid produced by EMQL showed better wettability and penetrability compared with the uncharged nanofluid, which enhanced the capillary penetration capacity of the Al₂O₃ nanofluid in the cutting interface and thus presented comparable tool wear, cutting force, and surface finish compared with the traditional oil-based MQL. Moreover, the PM 10 and PM 2.5 concentration and cutting temperature produced by Al₂O₃ fluid EMQL were much lower than the oil-based MQL, indicating that this kind of lubrication method can be a beneficial substitution for the traditional oil-based MQL. The excellent cutting performance of Al₂O₃ fluid EMQL was mainly because that the EMQL technology promoted a further penetration of the charged Al₂O₃ nanofluid to the cutting interface; the penetrated Al₂O₃ nanoparticles could act as ball bearings and serve as a medium to fill the grooves and concaves on the rubbing surface to prevent the interface from direct contact, which reduced friction force and cutting temperature obviously, and thus led to remarkable lubricating capacity. This water-based nanofluid EMQL technology has

been successfully applied to the double-sided milling machine produced by the Jiangsu Guda Machinery Co., Ltd. In addition, a cooperative relationship has been established with Jinyun Sawing Machine Manufacturer to provide this lubrication equipment in the circular saw machine. It is believed that this novel cleaner production process lubrication method could offer a promising industrial application and effective strategy for MQL.

Funding information This work was supported by the National Natural Science Foundation of China (Grant No. 51775507) and the Natural Science Foundation of Zhejiang Province (Grant No. LY19E050006).

References

- Wang YG, Li CH, Zhang YB, Yang M, Zhang XP, Zhang NQ, Dai JJ (2016) Experimental evaluation on tribological performance of the wheel/workpiece interface in minimum quantity lubrication grinding with different concentrations of Al_2O_3 nanofluids. *J Clean Prod* 142(4):3571–3583
- Cabanettes F, Faverjon P, Sova A, Dumont F, Rech J (2016) MQL machining: from mist generation to tribological behavior of different oils. *Int J Adv Manuf Tech* 90(1–4):1119–1130
- Junior ASA, Sales WF, Silva RB, Costa ES, Machado ARM (2017) Lubri-cooling and tribological behavior of vegetable oils during milling of AISI 1045 steel focusing on sustainable manufacturing. *J Clean Prod* 156(10):635–647
- Sharma AK, Tiwari AK, Dixit AR (2016) Effects of minimum quantity lubrication (MQL) in machining processes using conventional and nanofluid based cutting fluids: a comprehensive review. *J Clean Prod* 127(20):1–18
- Boswell B, Islam MN, Davies IJ, Ginting YR, Ong AK (2017) A review identifying the effectiveness of minimum quantity lubrication (MQL) during conventional machining. *Int J Adv Manuf Tech* 92(1–4):321–340
- Sharma VS, Singh GR, Sørby K (2015) A review on minimum quantity lubrication for machining processes. *Mater Manuf Process* 30(8):935–953
- Li BK, Li CH, Zhang YB, Wang YG, Jia DZ, Yang M, Zhang NQ, Wu QD, Han ZG, Sun K (2017) Heat transfer performance of MQL grinding with different nanofluids for Ni-based alloys using vegetable oil. *J Clean Prod* 154:1–11
- Wang YG, Li CH, Zhang YB, Yang M, Li BK, Jia DZ, Hou YL, Mao C (2016) Experimental evaluation of the lubrication properties of the wheel/workpiece interface in minimum quantity lubrication (MQL) grinding using different types of vegetable oils. *Tribol Int* 127:487–499
- Lin HS, Wang CY, Yuan YH, Chen ZH, Wang QM, Xiong WQ (2015) Tool wear in Ti-6Al-4V alloy turning under oils on water cooling comparing with cryogenic air mixed with minimal quantity lubrication. *Int J Adv Manuf Technol* 81(1–4):87–101
- Tai BL, Stephenson DA, Furness RJ, Shih AJ (2014) Minimum quantity lubrication (MQL) in automotive powertrain machining. *Proc CIRP* 14:523–528
- Leppert T (2012) Surface layer properties of AISI 316L steel when turning under dry and with minimum quantity lubrication conditions. *Proc Inst Mech Eng J Eng Manuf* 226(4):617–631
- Aoyama T, Kakinuma Y, Yamashita M, Aoki M (2008) Development of a new lean lubrication system for near dry machining process. *CIRP Ann-Manuf Techn* 57(1):125–128
- Lawal SA, Choudhury IA, Nukman Y (2013) A critical assessment of lubrication techniques in machining processes: a case for minimum quantity lubrication using vegetable oil-based lubricant. *J Clean Prod* 41:210–221
- MWFSAC (OSHA) (2008) Metalworking fluids safety and health best practice manual. Occupational safety & Health administration, Washington DC
- Gunter KL, Sutherland JW (1999) An experimental investigation into the effect of process conditions on the mass concentration of cutting fluid mist in turning. *J Clean Prod* 7(5):341–350
- Dunja DS, Hoflinger W, Sokolovic RMS, Sokolovic SM, Sakulski D (2013) Experimental study of mist generated from metalworking fluids emulsions. *J Aerosol Sci* 61:70–80
- Itoigawa F, Childs THC, Nakamura T, Belluco W (2006) Effects and mechanisms in minimal quantity lubrication machining of an aluminum alloy. *Wear* 260(3):339–344
- Mao C, Zhang J, Huang Y, Zou HF, Huang XM (2013) Investigation on the effect of nanofluid parameters on MQL grinding. *Mater Manuf Process* 28(4):436–442
- Ii M, Eda H, Imai T, Nishimura M, Kawasaki T, Shimizu J, Yamamoto T, Zhou L (2000) Development of high water-content cutting fluids with a new concept: Fire prevention and environmental protection. *Precis Eng* 24(3):231–236
- Setti D, Sinha MK, Ghosh S, Rao PV (2015) Performance evaluation of Ti-6Al-4V grinding using chip formation and coefficient of friction under the influence of nanofluids. *Int J Mach Tool Manu* 88:237–248
- Najiha MS, Rahman MM (2016) Experimental investigation of flank wear in end milling of aluminum alloy with water-based TiO_2 nanofluid lubricant in minimum quantity lubrication technique. *Int J Adv Manuf Technol* 86(9–12):2527–2537
- Zhang YB, Li CH, Ji HJ, Yang XH, Yang M, Jia DZ, Zhang XP, Li RZ, Wang J (2017) Analysis of grinding mechanics and improved predictive force model based on material-removal and plastic-stacking mechanisms. *Int J Mach Tool Manu* 122:81–97
- Yang M, Li CH, Zhang YB, Jia DZ, Zhang XP, Hou YL, Li RZ, Wang J (2017) Maximum undeformed equivalent chip thickness for ductile-brittle transition of zirconia ceramics under different lubrication conditions. *Int J Mach Tool Manu* 122:55–65
- Lv T, Huang SQ, Hu XD, Ma YL, Xu XF (2018) Tribological and machining characteristics of a minimum quantity lubrication (MQL) technology using GO/SiO₂ hybrid nanoparticle water-based lubricants as cutting fluids. *Int J Adv Manuf Technol* 96(5–8):2931–2942
- Huang SQ, Wang Z, Yao WQ, Xu XF (2015) Tribological evaluation of contact-charged electrostatic spray lubrication as a new near-dry machining technique. *Tribol Int* 91:74–84
- Huang SQ, Lv T, Xu XF, Ma YL, Wang MH (2018) Experimental evaluation on the effect of electrostatic minimum quantity lubrication (EMQL) in end milling of stainless steels. *Mach Sci Technol* 22(2):271–286
- Huang SQ, Lv T, Wang MH, Xu XF (2018) Enhanced machining performance and lubrication mechanism of electrostatic minimum quantity lubrication-EMQL milling process. *Int J Adv Manuf Tech* 94(1–4):655–666
- Xu XF, Huang SQ, Wang MH, Yao WQ (2017) A study on process parameters in end milling of AISI-304 stainless steel under electrostatic minimum quantity lubrication conditions. *Int J Adv Manuf Technol* 90(1–4):979–989
- Huang SQ, Lv T, Wang MH, Xu XF (2018) Effects of machining and oil mist parameters on electrostatic minimum quantity lubrication-EMQL turning process. *Int J Pr Eng Man-GT* 5(2):317–326
- Reddy NSK, Yang M (2010) Development of an electro static lubrication system for drilling of SCM 440 steel. *Proc Inst Mech Eng J Eng Manuf* 224(2):217–224

31. Reddy NSK, Nouari M, Yang M (2010) Development of electrostatic solid lubrication system for improvement in machining process performance. *Int J Mach Tools Manuf* 50(9):789–797
32. Su Y, Gong L, Bi L, Liu ZQ, Chen DD (2016) Performance evaluation of nanofluid MQL with vegetable-based oil and ester oil as base fluids in turning. *Int J Adv Manuf Technol* 83(9–12):2083–2089
33. Chatha SS, Pal A, Singh T (2016) Performance evaluation of aluminium 6063 drilling under the influence of nanofluid minimum quantity lubrication. *J Clean Prod* 137:537–545
34. Zhao W, Ning H, Liang L, Yang YF, Shi Q (2014) Investigation on the influence of system parameters on ambient air quantity in minimum quantity lubrication milling process. *J Mech Eng-En* 50(13): 184–189
35. Zhao ZN (2008) Heat transfer. Higher Education Press, Beijing
36. Jones AR, Thong KC (1971) The production of charged monodisperse fuel droplets by electrical dispersion. *J Phys D Appl Phys* 4(8):1159–1166
37. Godlevski VA, Volkov AV, Latyshev VN, Maurin LN (2010) The kinetics of lubricant penetration action during machining. *Lubr Sci* 9(2):127–140
38. Young T (1805) An essay on the cohesion of fluids. *Philos Trans R Soc Lond* 95:65–87
39. Gao SQ, Liu HP (2010) Capillary mechanics. Science Press, Beijing
40. Luo HC (1990) Practical manual of electrostatic technology. Shanghai science popularization press, Shanghai
41. Marano RS (1997) Polymer additives as mist suppressants in metal cutting fluids. *Lub Eng* 53(10):25–36
42. Smolinski JM, Gulari E, Manke CW (1996) Atomization of dilute polymer additives as mist suppressants in metal cutting fluids. *AICHE J* 42(5):1201–1202
43. Behera BC, Chetan SD, Ghosh S, Rao PV (2017) Spreadability studies of metal working fluids on tool surface and its impact on minimum amount cooling and lubrication turning. *J Mater Process Technol* 244:1–16
44. Shen B, Shih AJ, Tung SC (2008) Application of nanofluids in minimum quantity lubrication grinding. *Tribol T* 51(6):730–737
45. Emami M, Sadeghi MH, Sarhan AAD (2013) Investigating the effects of liquid atomization and delivery parameters of minimum quantity lubrication on the grinding process of Al₂O₃ engineering ceramics. *J Manuf Process* 15(3):374–388
46. Tawakoli T, Hadad MJ, Sadeghi MH (2010) Influence of oil mist parameters on minimum quantity lubrication-MQL grinding process. *Int J Mach Tools Manuf* 50(6):521–531
47. Jawaid A, Sharif S, Koksai S (2000) Evaluation of wear mechanisms of coated carbide tools when face milling titanium alloy. *J Mater Process Technol* 99(1–3):266–274

Publisher's note Springer Nature remains neutral with regard to jurisdictional claims in published maps and institutional affiliations.